Tracking the space debris from the Changchun Observatory

Zhipeng Liang[1] · Xue Dong[1] · Makram Ibrahim[2] · Qingli Song[1] · Xingwei Han[1,3] · Chengzhi Liu[1] · Haitao Zhang[1] ·
Guohai Zhao[1]

Abstract Changchun Observatory tracked Space Debris since Feb. 2014. This paper presents the technologies and results of Changchun station for space debris laser ranging (DLR) system. The system operates with a laser of 60 mJ/10 ns/500 Hz@532 nm laser and an optical camera for closed-loop tracking. Target selection assistant was introduced to DLR system. To represent the probability of return, the rebound index was calculated. Data identification was implemented in tracking control software and data processing. To improve the return rate, Range Bias/Time Bias is auto-corrected in the tracking software. The aim of this paper is to show the results and the analysis of the space debris observed during the period from the year 2014 to the year 2016. There are 491 passes observed for 232 different space debris targets were obtained during 35 terminator sessions. The observed targets are ranging between 460 km to 1800 km, with Radar Cross Sections (RCS) from > 15 m^2 to < 1.0 m^2. The Root Mean Square (RMS) value of the range is measured to be less than 1 m for small targets, due to the 10 ns laser pulse length while for large objects it can reach up to 3.5 meters.

✉ M. Ibrahim
makikh@yahoo.com

[1] Changchun Observatory of National Astronomical Observatories, CAS, Changchun, China

[2] National Research Institute of Astronomy and Geophysics, Helwan 11421, Cairo, Egypt

[3] Key Laboratory of Space object and Debris Observation, Purple Mountain Observatory, CAS, Nanjing, China

1 Introduction

The laser ranging technique is considered to be one of the most accurate methods to track the artificial earth satellites (Pearlman et al. 2002). The primary goal of the satellite laser ranging is the measurement of the time required for pulses emitted by a laser transmitter to travel to a satellite and return back to the transmitting site. The "range", or distance between the satellite and the tracking site, is approximately one half of the two—ways travel time multiplied by the speed of light. A lot of work deals with the satellite laser ranging technique (Cech et al. 1998; Zhao et al. 2008; Ibrahim 2011; Ibrahim et al. 2015).

In Changchun observatory, the daytime tracking started at 11 am of May 16th, 2008. It is carried out by updating the original system to adapt the new technology for daylight KHz (Zhao et al. 2006; Yang et al. 1999; Han et al. 2013). The Changchun station started the space debris laser ranging at the end of 2013, using the 60 cm aperture laser ranging system. The aim of this paper is to discuss the space debris laser ranging from the Changchun observatory. One of the main applications of the data is to prepare a database for the space debris. Such database will be very useful for the newly launched satellites as well as to keep the working satellites away from the collision with the space debris. The data was not used for precise prediction because it was too sparse for most targets. It is single-station that works only on twilight time. On the other hand, there is a cooperation between NRIAG of Egypt and the NAOC (Changchun Observatory) of China, in the field of the satellite and the space debris laser ranging. For this end, the data produced from both sides can be used for more precise orbit predictions. For science use, these data are used for solving the reflection parameter.

For this end we explained the satellite laser ranging from the Changchun station in Sect. 2. In Sect. 3, we discussed

Fig. 1 The 60 cm telescope at Changchun Observatory

Table 1 Primary parameters of ns-laser

Performances	ns-laser
Working mode	Laser diode pump
Wavelength	532 nm
Repetition rate	1–500 Hz adjustable
Pulse energy	60 mJ@500 Hz
M^2 factor	≤1.5
Pulse width	9–10 ns
Beam divergence	0.4 mrad
Beam divergence after the transmit telescope	22 µrad

the work in the system used for the debris laser ranging. In Sect. 4 the tracking technologies used in Changchun observatory will be discussed. Finally, the observational data and the results are presented in Sect. 5.

2 Satellite Laser Ranging (SLR) in Changchun

The Changchun satellite laser ranging system uses a computer controlled azimuth/elevation mount for telescope pointing. The mount movement is driven by separate azimuth and elevation direct-drive motors, with maximum slew rate of 5 deg./sec. The pointing precision is 1 arcsec with pointing accuracy of about 5 arcsec after star calibration. The transmitter is a 20 centimeter refractor telescope, while the receiver is 60 centimeter aperture R-C reflector telescope, as shown in Fig. 1.

The type of detector is a compensated single photon avalanche diode (C-SPAD) made by the Czech Technical University. The quantum efficiency of this C-SPAD is 20% at 532 nm wavelength. It works in Geiger mode to detect single photon echoes (Zhao et al. 2008).

The laser source is a Nd:YAG solid state Q-switched laser, manufactured by Photonics Industries. The output pulse energy is one millijoule at 532 nm of wavelength and with a pulse width of 50 Pico second (FWHM). The laser is set to repeat one thousand times per second while ranging to satellites, making output power of one watt. The beam divergence is 0.4 mrad at laser chamber, and directed through coude paths and compressed to 22 µrad via transmitter telescope.

An event timer A-033ET is used for laser roundtrip time measurement (Fan et al. 2006). Its nominal resolution is better than 10 ps. For time standard, an Endrun Meridian II time base is used to provide 1pps and 10 MHz UTC epoch signals with accuracy better than 100 ns. For environment parameters, MET3 meteorological measurement system manufactured by Paroscientific Inc. is used. It measures atmospheric pressure with a precision up to 0.08 mbar, and temperature to 0.1 degrees Celsius, and measuring relative humidity with 1% precision.

3 Debris Laser Ranging (DLR) in Changchun

Changchun station planned to begin the space debris laser ranging at the end of 2013, which based on Changchun 60 cm aperture laser ranging system. Aiming at a series of problems such as space debris objects' angular rate, prediction accuracy and signal identification, high precision, high sensitivity, and high automation, the observation was effective. The space debris laser ranging (DLR) system with high repetition rate had been established. The laser measurements to space debris are also studied at the Graz SLR station (Kirchner and Koidl 2004; Kirchner et al. 2013).

The DLR system was arranged in parallel with the SLR system. The equipments used in the DLR system almost the same equipments of SLR system except for a ns-laser. The ns-laser is placed beside ps-laser, switched by a moveable mirror to allow the ns-laser to pass through or direct the kHz ps-laser (for SLR) to the coudé path. The main performances of ns-laser are listed in Table 1. We would like to mention that, due to weak TLE predictions, the debris laser ranging needs optical feedback. This means that all the measurements have been done only during terminator periods (target in sunlight, station in darkness).

4 Tracking technologies used in Changchun Observatory

New tracking technologies were used in the debris laser ranging system, such as tracking control program upgrade, rebound index calculation, space debris data base establishment, closed-loop tracking, target quick search, and range bias improvement and signal recognition and noise filtering.
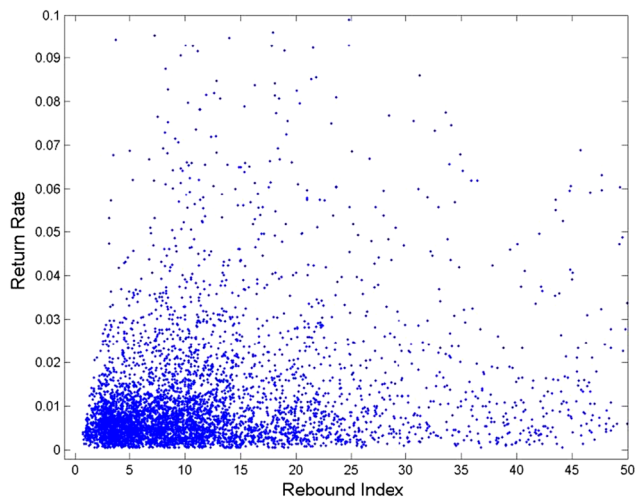
Fig. 2 The rebound index vs. the return rate from space debris tracking

4.1 Upgrade tracking control program

In order to get effective data, a serial of operations were done on the DLR software systems (Zhao et al. 2008).

4.2 Rebound index calculation

To estimate the strength of laser pulse rebounded by a given space debris target, the rebound index is used. It is a dimensionless number calculated as in the following equation:

$$I_{rebound} = \frac{S/S_0}{(R/R_0)^4} \tag{1}$$

where S is cross section area of the given space debris target, and S_0 is reference area, which is one square meter. R is the range to the space debris target, and R_0 is the reference range, which is 1000 kilometer. We choose one square meter target at 1000 km range as reference scenario, and the rebound index $I_{rebound}$ shows how many times of reference echo strength would be obtained.

This formula is model-based and never be validated with data. But from the analysis of raw data, we can give realtime return rate. Comparison between return rate and rebound index will give some validation of the formula as shown in Fig. 2. For some reasons, the return rates for same targets are different. The return rate will vary with distance (range) and more factors such as the shape and attitude of target will also affect the return rate.

The return rate can be calculated using the following equation:

$$K_{RR} = \frac{N_R}{N_S} \tag{2}$$

where, K_{RR} is return rate, N_R is the number of returned photons and N_S is the number of laser shots. In this work, the return rate is calculated from CRD normal point records of the SD objects. In the CRD normal point ('11') records, both normal point window length and number of selected raw ranges are recorded (Ricklefs 2009). With the time window length, we can calculate the total number of laser pulses, by multiplying window length and firing repetition rate. We can estimate the number of photons that return from SD object with the number of selected raw ranges.

As for the reflectivity of targets, it is possible to compute it from the return rate. It can be computed from the incident laser illumination on the target, and the reflected illumination from the target of the return rate as explained in the Appendix.

4.3 Space debris database establishment

As it is extremely difficult to track space debris objects, due to both of their small cross section and their short passing time, we planned to track the targets with the orbit height of about 1000 km, Radar Cross Section (RCS) larger than 1 m^2, and easier to track under our own estimation.

The target assistant software was developed, including the automatic updates of the Two Line Element (TLE) and target selection. The interface of target selection assistant software is shown in Table 2. Space debris could be selected by target type, RCS, pass maximum elevation, and rebound index, we could select targets we need and download the TLE prediction files onto local computer disk for use. This software saved much time in selecting target to track, while improving detection rate.

4.4 Closed-loop tracking

The closed-loop tracking technique with CCD image is developed to ensure the target in the center of view. On a given epoch, the CCD device snaps an image containing target and laser beam tip, and coincidentally passing stars. The composite image is analyzed by software to extract target position offset. The offset is then feedback to tracking computer, so that to keep the target in a reference point in FOV.

4.5 Graphical operation interface

Because the space debris target has relatively high angular rate and poor prediction accuracy, the ranging control software has provided a graphical operation interface to help user to handle the tracking and ranging process (Zhao et al. 2008).

4.6 Range bias improvement

As the range bias of TLE prediction could be up to a few hundred meters, it is necessary to improve the orbit prediction. We developed a method to calculate the real-time

Table 2 Sample of the space debris database display

Date	Begin	End	Max. Elv.	Rebound index	NORAD ID	RCS area	Name	Orbital altitude/km
13/5/2014	00:00	00:07	86 deg.	12.1	20855	7.3 m^2	CZ-4 DEB	864 km
13/5/2014	00:00	00:11	63 deg.	7.3	8520	6.5 m^2	SL-3 R/B	863 km
13/5/2014	00:01	00:09	69 deg.	5.7	8546	0.1 m^2	SL-12 R/B (Aux Motor)	10463 km
13/5/2014	00:01	00:10	56 deg.	13.1	19211	4.1 m^2	SL-14 R/B	621 km
13/5/2014	00:02	00:12	57 deg.	9.6	16953	6.5 m^2	SL-8 R/B	768 km
13/5/2014	00:02	00:13	76 deg.	21.0	19120	10.5 m^2	SL-16 R/B	828 km
13/5/2014	00:02	00:11	67 deg.	18.8	15370	4.2 m^2	SL-14 R/B	620 km
13/5/2014	00:03	00:11	75 deg.	86.6	28813	9.9 m^2	SL-24 R/B	554 km
13/5/2014	00:07	00:13	28 deg.	11.6	11849	5.4 m^2	SL-3 R/B	434 km
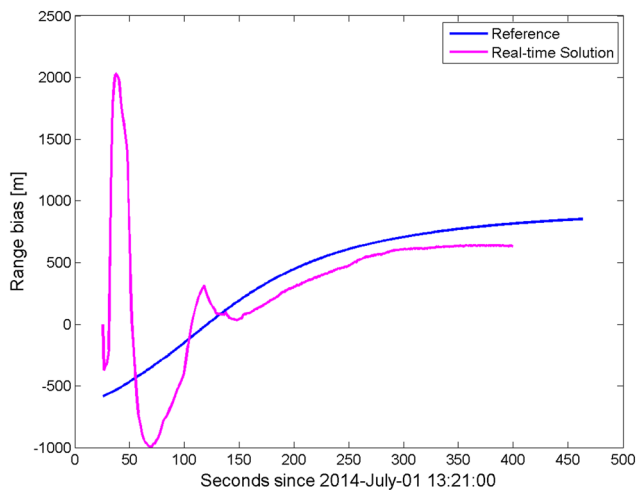
Fig. 3 Real-time range bias improvement using position bias

range difference according to real-time visual position off-set, which could improve the prediction accuracy to less than a hundred meters in a few minutes. The results were shown in Fig. 3, which represented for the satellite Envisat that had CPF ephemeris as reference orbit. It can be seen in the graph that, although the solution fluctuated in the first minute, it converged to the reference range bias.

4.7 Signal recognition and noise filtering

The data recognition technique is used to pick the real return signals from the kilo-hertz signal stream, therefore filtering noise signals. This technique, was first proposed by (Kirchner and Koidl 2004).

In the Changchun system, this recognition is applied two times for each pass. The first time is during tracking operation, for operators to know if target is in the scope. This stage requires real-time performance. The second time is when the raw data file is loaded by data-processing software. The data-processing computer, with a better computation power,

will make more sophisticated comparisons to ensure noise events are excluded. This technique reduces significantly the need to manually process data.

Figure 4, shows an example for the data recognition. The target is space debris SL-16 rocket stage, with TLE number 25400. The data was taken in year 2014, April 11th, 19h UTC. The two gaps in this figure are caused by overlap of the transmitted and received packets (Tx-Rx). At the time of experiment, the laser did not support firing epoch control, so we let it run on internal trigger. It does not affect the validity of the measurements.

## 5 Observational data and results

During the period from year 2014 to year 2016, 491 passes were observed of 232 space targets within elevation from 19° to 87°. Sample of the data observed for the space debris with NORAD ID # 25400 is given in Table 3. The number of normal points per pass for each passes of space target is shown in Fig. 5. We would like to mention that the number of points per normal point is the number of valid echoes collected during 5 seconds of tracking. The distribution of the observed space debris according to the range distance and the radar cross sections (RCS) is shown in Fig. 6. It is clear that the range distance varies from 460 km to 1800 km and the RCS varies from 26 m^2 to 0.75 m^2. We scheduled 35 terminator (twilight) tracking sessions in 26 days. The distribution of the observed space debris according to their altitudes and according to the countries is shown in Fig. 7. Figure 8 shows the distribution of the observed space debris according to the tracking time as in (a) and according to the orbit inclination in (b). The Root Mean Square value of the range is computed for each pass and the results is shown in Fig. 9.

The root mean square values are computed as a function of the space debris RCS and the results are shown in Fig. 10. We computed the average value of the RMS for each space

Fig. 4 Sample of data recognition or noise filtering method, before filtering in (**a**) and after filtering in (**b**)
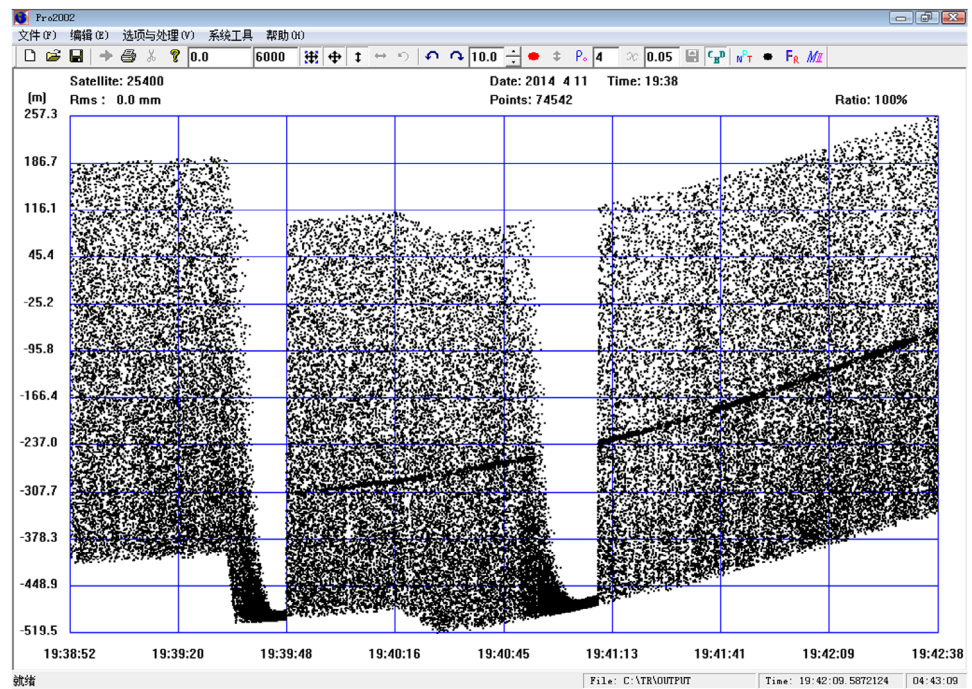
(a)
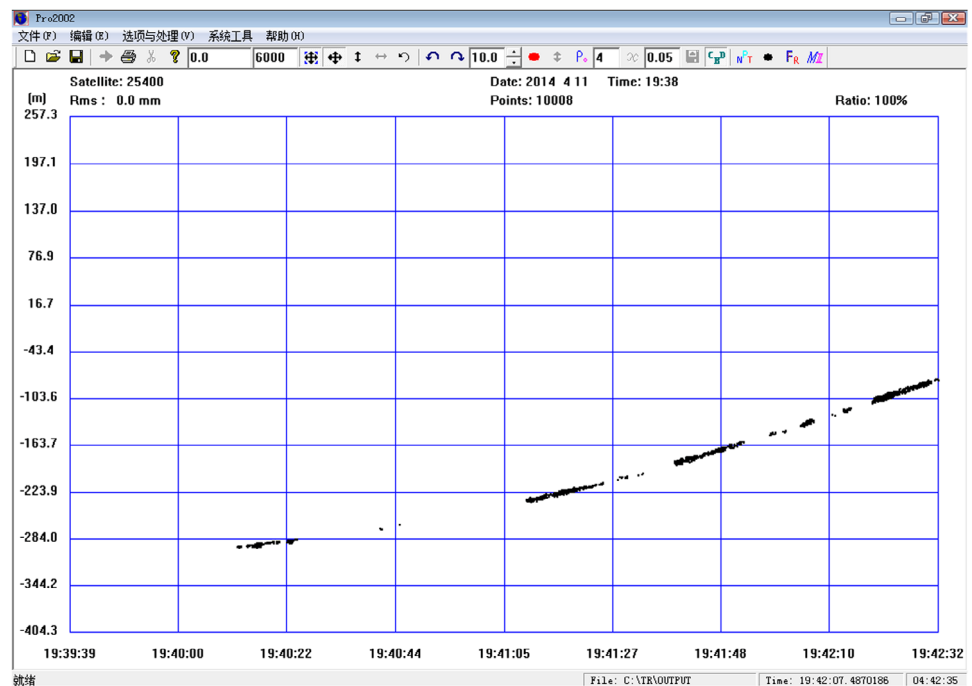
(b)

debris object. It is clear that the errors of range are bigger when the size of the space debris are bigger and vice versa.

6 Conclusion

Changchun observatory tracked space debris since Feb. 2014. This paper presented the technologies and results of Changchun station for space debris laser ranging (DLR). From year 2014 to the year 2016, there are 491 passes of 232 different space debris targets were acquired with elevations between 19° to 87°. The space debris target distances are ranging between 460 km to 1800 km, with Radar Cross Sections (RCS) varying from 26 m^2 to 0.75 m^2. There are up to 67 passes acquired in a single day and record 36 passes

Table 3 Sample of the debris laser ranging data

2014 04 11 9804307 (NORAD ID# 25400)

$T = 275.50$ K; $H = 63\%$; $P = 987.0$ mbar

Second of day	Measured range (ms)	Range rate (km/s)	hhmmss	Azimuth angle (deg)	Elevation angle (deg)
70956.30516	7.58644428	1.158224	194236.3052	111.8236	41.6957
70956.30916	7.585652428	1.158394	194236.3092	111.8255	41.6955
70956.31116	7.586564006	1.158479	194236.3112	111.8265	41.6953
70956.31316	7.588039727	1.158564	194236.3132	111.8275	41.6952
70956.31516	7.585989967	1.158649	194236.3152	111.8285	41.6951
70956.32116	7.587291219	1.158904	194236.3212	111.8315	41.6947
70956.32716	7.585325138	1.159159	194236.3272	111.8344	41.6943
70956.33116	7.585569358	1.159328	194236.3312	111.8364	41.694
70956.33516	7.585571757	1.159498	194236.3352	111.8384	41.6937
70956.33717	7.58539421	1.159583	194236.3372	111.8394	41.6936
70956.33917	7.586690115	1.159668	194236.3392	111.8404	41.6935
70956.34117	7.585559789	1.159753	194236.3412	111.8414	41.6933
70956.34317	7.585448717	1.159838	194236.3432	111.8424	41.6932
70956.34917	7.586091908	1.160093	194236.3492	111.8453	41.6928
70956.35117	7.587248058	1.160178	194236.3512	111.8463	41.6927
70956.35317	7.58595033	1.160263	194236.3532	111.8473	41.6925
70956.35917	7.58759873	1.160517	194236.3592	111.8503	41.6921
70956.36117	7.585881329	1.160602	194236.3612	111.8513	41.692

Fig. 5 The normal point numbers per pass observed during the period from year 2014 to year 2016
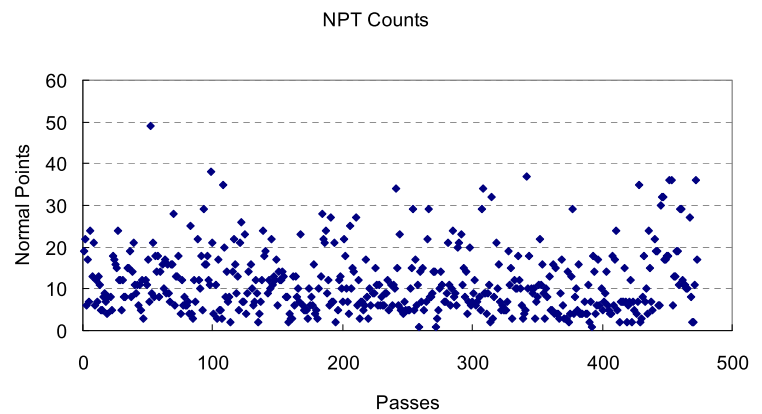

Fig. 6 The distribution of the observed space debris according to the range distribution in (**a**) and according to the RCS in (**b**)
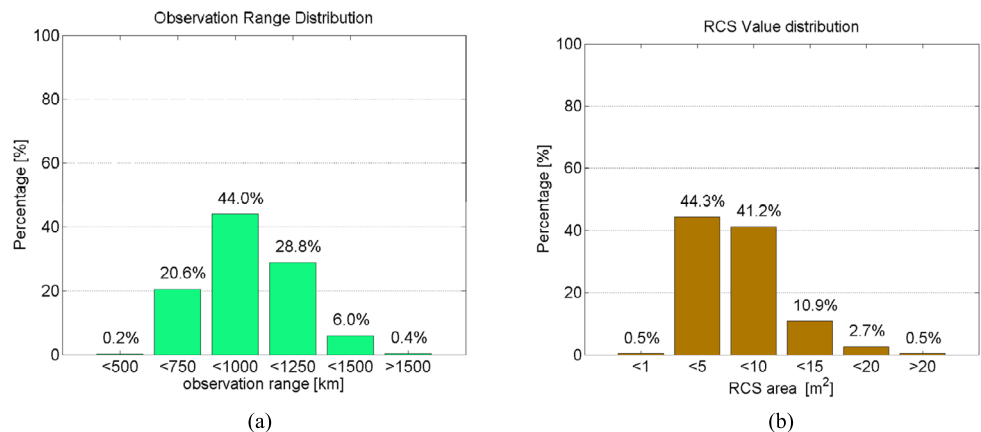

(a)

(b)

Fig. 7 The distribution of the observed space debris according to the Altitude distribution in (**a**) and according to the countries in (**b**)
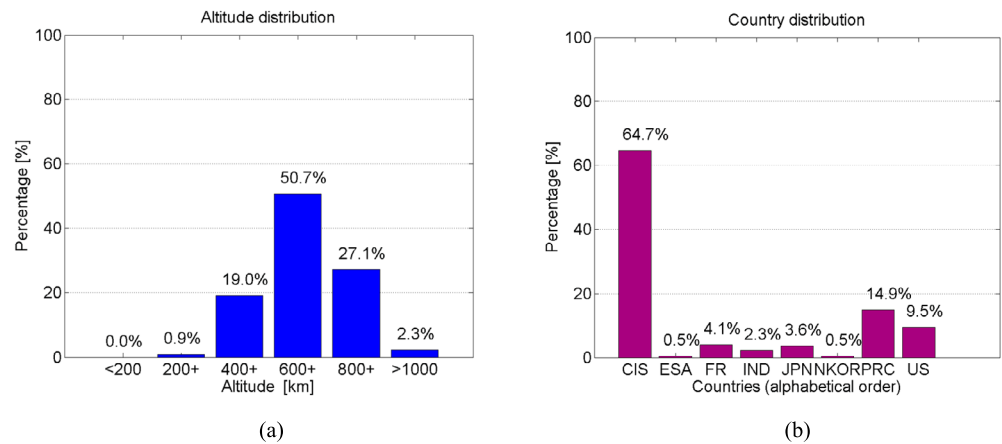

(a)

(b)

Fig. 8 The distribution of the observed space debris according to the tracking time distribution in (**a**) and according to the orbit inclination in (**b**)
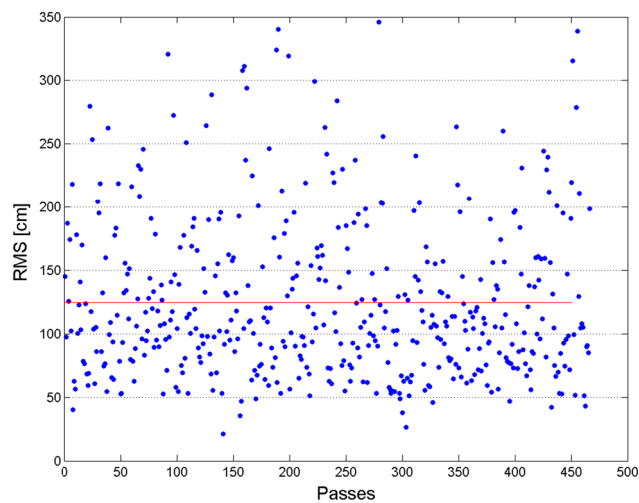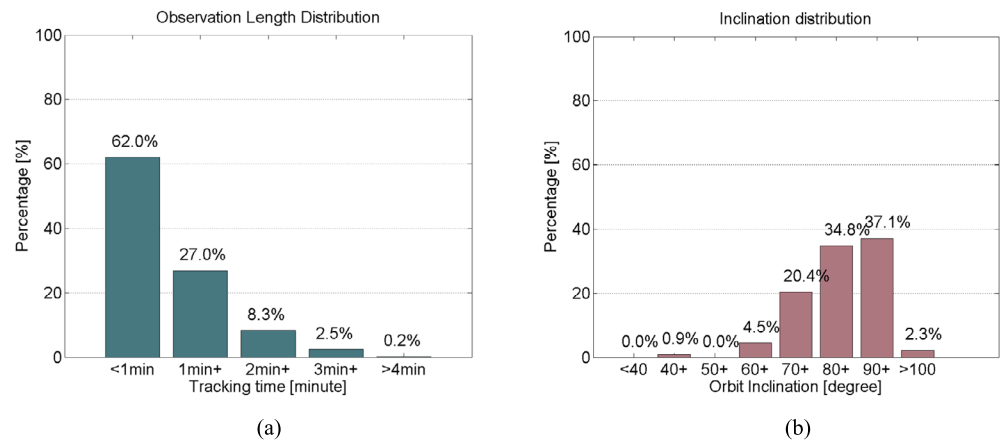

(a)

(b)

Fig. 9 Precision (RMS) of Passes distribution

Fig. 10 RMS values of range measurements vs. the target RCS

was obtained in one twilight session during the period of tracking. The Root Mean Square (RMS) value of the range is measured to be less than 1 m for small targets, due to the 10 ns laser pulse length while for large objects it can reach 3.5 meters. For some reasons, the return rates for same targets are different. The return rate will vary with distance
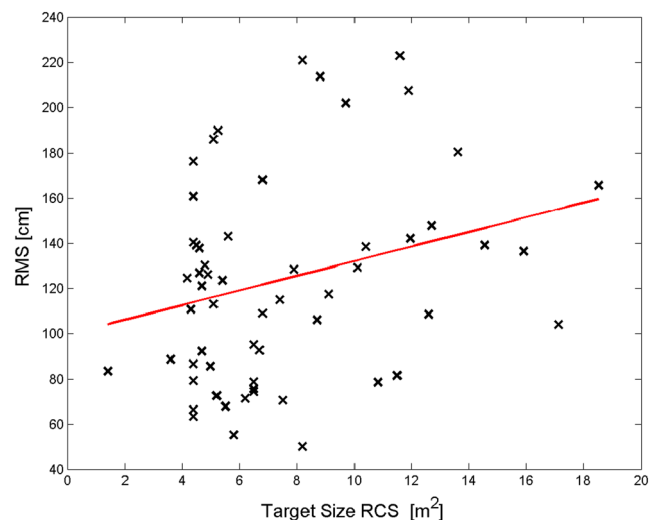
(range) and more factors such as the shape and attitude of target.

Appendix: The reflectivity of the targets

In the of a laser ranging system, the number of received photoelectrons on one shot can be computed from the following formula (Degnan 1985):

$$N_{pe} = \eta_q E_T \frac{\lambda}{hc} \eta_T G_T \left(\frac{1}{4\pi}\right)^2 A_T \eta_R T_A^2 T_C^2 \cdot \frac{\sigma}{R^4} \tag{3}$$

We separate target optical area σ and target range R, for further transformation.

Note that the formula of rebound index, we have:

$$N_{pe} = \eta_q E_T \frac{\lambda}{hc} \eta_T G_T \left(\frac{1}{4\pi}\right)^2 A_T \eta_R T_A^2 T_C^2 \cdot \frac{\sigma_0}{R_0^4}$$
$$\cdot \frac{k\sigma_{RCS}/\sigma_0}{R^4/R_0^4} \tag{4}$$

$$N_{pe} = \eta_q E_T \frac{\lambda}{hc} \eta_T G_T \left(\frac{1}{4\pi}\right)^2 A_T \eta_R T_A^2 T_C^2 \cdot \frac{\sigma_0}{R_0^4}$$
$$\cdot k \cdot I_{rebound} \tag{5}$$

where we further separate target optical area σ to be reflectivity k times σ_{RCS}, since target's effective area of reflection varies with time, while its RCS area is stable. The reflectivity k should be less than 1.

Finally, Eq. (5) that relates the return photoelectron and the rebound index. The return rate is a statistical estimation of N_{pe}. When N_{pe} is sufficiently small (< 0.1), the return rate is equivalent to N_{pe}. So we get a relation between return rate and rebound index.

$$\text{Return Rate} = \eta_q E_T \frac{\lambda}{hc} \eta_T G_T \left(\frac{1}{4\pi}\right)^2 A_T \eta_R T_A^2 T_C^2 \cdot \frac{\sigma_0}{R_0^4}$$
$$\cdot k \cdot I_{rebound} \tag{6}$$

From the definition of the return rate which can be calculated as the Number of returned photoelectrons divided by the number of laser pulses. For the right hand side of the formula, the first part is rather stable. We call it unit photoelectron of the system: N_{upe}. For the Changchun system, the value of N_{upe} can be calculated as: $N_{upe} = 0.01$ (where the SPAD quantum efficiency $\eta_q = 20\%$; pulse energy $E_T = 60$ mJ; wavelength $= 532$ nm; Planck's constant $= 6.63E\text{-}34$; speed of light $= 299792458$ m/s; transmit efficiency $\eta_T = 0.7$; transmit gain $G_T = 1732291625$, where laser spread angle is 22 μrad; receiver aperture area $= 0.25$ m^2 for 60 cm telescope; receive efficiency $\eta_R = 0.7$; Atmospheric Transmission $T_A = 0.4$; Cirrus Cloud Transmission ignored, making $T_C = 1$; target area $\sigma_0 = 1$ m^2 for unit area; target range $R = 1000$ km for unit range).

Its meaning is the number of photoelectrons to record when the Changchun system fires a pulse to a 1 m^2 ideal target located 1000 km away. Ideal means 100% reflection.
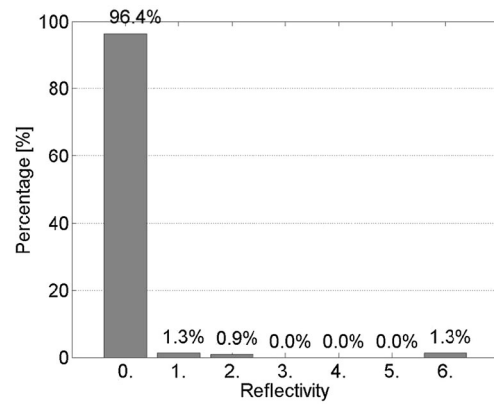

Fig. 11 The reflection from the space debris objects

The second part is reflectivity k, which varies by time during laser ranging. The third part is the rebound index that can be calculated by normal point ranges and target RCS parameter. The above formula has one unknown variable which is k the reflectivity. It can be calculated with:

$$k = \frac{N_{pe}}{N_{upe} \cdot I_{rebound}} \tag{7}$$

The reflectivity for each target is calculated, and the results are given in the following histogram (see Fig. 11).

Note that most of target reflectivity are very small. Some of them exceed 1, and others can reach even more than 6.9, which is anomalous. These targets are: The target of ID (11327) has a reflectivity of 6.99, of ID (31114) has a reflectivity of 6.97, of ID (28480) has a reflectivity of 6.16, of ID (22220) has a reflectivity of 2.27, and of ID (23324) has a reflectivity of 2.03.

The underestimate of N_{upe} could lead to overestimate of reflectivity. The cause of anomaly needs further investigation. However, some of the above targets are known to have reflectors onboard (Liang et al. 2016), this could partly explain the high reflectivity.

References

Cech, M., Hamal, K., Jelinkova, H., Novotny, A., Prochazka, I., Helali, Y.E., Tawadros, M.Y.: Upgrading of the Helwan laser station (1997–1998). In: Proceedings of the 11th International Workshop on Laser Ranging, Deggendorf, Germany, pp. 197–200 (1998)

Degnan, J.: Millimeter Accuracy Satellite Laser Ranging: A Review. AGU Geodynam Ser., vol. 25, pp. 133–162. Springer, Berlin (1985)

Fan, C., Dong, X., Zhao, Y., Han, X.: A023-ET experimental test on Changchun SLR. In: Proceedings of 15th International Laser Ranging Workshop, Canberra, Australia, Oct. 15–21, 2006 pp. 300–305 (2006)

Han, X., Dong, X., Song, Q., Zhang, H., Shi, J.: Fulfillment of KHz SLR daylight tracking of Changchun Station. In: Proc. of 17th ILRS Meeting, Fujiyoshida, Japan, November 11–15 (2013)

Ibrahim, M.: 17 years of ranging from the Helwan-SLR station. Astrophys. Space Sci. **335**, 379–387 (2011)

Ibrahim, M., Yousry, S.H., Samwel, S.W., Marawan, M.: Satellite laser ranging in Egypt. NRIAG J. Astron. Geophys. **4**, 123–129 (2015)

Kirchner, G., Koidl, F.: Graz KHz SLR system: design, experiences and results. In: 14th International Workshop on Laser Ranging, San Fernando, Spain, June 7–11 (2004)

Kirchner, G., Koidl, F., Friederich, F., Buske, I., Volker, U., Riede, W.: Laser measurements to space debris from Graz SLR station. Adv. Space Res. **51**(1), 21–24 (2013)

Liang, Z., Han, X., Fan, C., Liu, C.: Laser ranging observation and orbit determination of rotating reflective CZ-2C rocket stage. In: Proc. of 20th Int. Workshop on Laser Ranging, Potsdam, Germany, October 9–14 (2016)

Pearlman, M.R., Degnan, J.J., Bosworth, J.M.: The international laser ranging service. Adv. Space Res. **30**(2), 135–143 (2002)

Ricklefs, R.L.: Consolidated Laser Ranging Data Format (CRD) Version 1.01 (2009). https://ilrs.cddis.eosdis.nasa.gov/docs/2009/crd_v1.01.pdf

Yang, F., Xiao, Z., Cen, W., et al.: Design and observations of the satellite laser ranging system for daylight tracking at shanghai observatory. Sci. China Ser. A **42**(2), 198–206 (1999)

Zhao, Y., Han, X., Fan, C.B., Dai, T.: Fulfillment of SLR daylight tracking of Changchun station. In: Proceedings of 15th International Laser Ranging, Workshop, Canberra, Australia, Oct. 15–21, 2006, pp. 587–592 (2006)

Zhao, Y., Fan, C.B., Han, X.W., Zhao, G., Zhang, Z., Dong, X., Zhang, H.T., Shi, J.Y.: Progress in Changchun SLR. In: Proceedings of the 16th International Workshop on Laser Ranging, Poznan, Poland, pp. 525–530 (2008)